Probing the Conformation of the Fibronectin III$_{1-2}$ Domain by Fluorescence Resonance Energy Transfer*$^{\boxed{S}}$

Nancy W. Karuri[1], **Zong Lin, Hays S. Rye, and Jean E. Schwarzbauer**[2]

From the Department of Molecular Biology, Princeton University, Princeton, New Jersey 08544-1014

Fibronectin (FN) matrix is crucial for cell and tissue functions during embryonic development, wound healing, and oncogenesis. Assembly of FN matrix fibrils requires FN domains that mediate interactions with integrin receptors and with other FN molecules. In addition, regulation of FN matrix assembly depends on the first two FN type III modules, III$_1$ and III$_2$, which harbor FN-binding sites. We propose that interactions between these two modules sequester FN-binding sites in soluble FN and that these sites become exposed by FN conformational changes during assembly. To test the idea that III$_{1-2}$ has a compact conformation, we constructed CIIIY, a conformational sensor of III$_{1-2}$ based on fluorescent resonance energy transfer between cyan and yellow fluorescent proteins conjugated at its N and C termini. We demonstrate energy transfer in CIIIY and show that fluorescent resonance energy transfer was eliminated by proteolysis and by treatment with mild denaturants that disrupted intramolecular interactions between the two modules. We also show that mutations of key charged residues resulted in conformational changes that exposed binding sites for the N-terminal 70-kDa FN fragment. Collectively, these results support a conformation-dependent mechanism for the regulation of FN matrix assembly by III$_{1-2}$.

Fibronectin (FN)[3] is a 500-kDa modular dimeric protein and a major component of the extracellular matrix. It exists in the blood and other body fluids as a soluble compact molecule and undergoes cell-mediated assembly to form an insoluble three-dimensional fibrillar matrix (reviewed in Ref. 1). The process of FN matrix assembly has been implicated in embryonic development, wound healing, and cancer (2–4). FN is composed of type I–III modules, and sets of these modules comprise binding domains for cells and for other extracellular matrix components (see Fig. 1A). Three of these binding domains are essential

for matrix assembly (1). Integrin receptor interactions with the cell-binding domain tether disulfide-bonded FN dimers to the cell surface, where FN-FN interactions involving the N-terminal assembly domain form dimers into fibrils. In addition to these essential domains, other FN-binding sites have been implicated in assembly. In particular, the III$_{1-2}$ FN-binding domain plays a regulatory role in matrix assembly. Within this domain reside a cryptic FN-binding site in III$_1$ and a site available for FN binding in the native form of III$_2$ (5–8). Recombinant FN lacking III$_1$ is assembled into a matrix at wild-type levels, but that lacking the III$_{1-2}$ domain results in short immature FN fibrils (8). Peptides derived from the III$_{1-2}$ domain or antibodies against III$_{1-2}$ block matrix assembly by cultured cells (9–11). Furthermore, FN binding to this region is enhanced when FN is mechanically stretched (12). Taken together, these results suggest that conformational changes in the III$_{1-2}$ domain may control its interactions during FN assembly.

To more fully understand the roles of native and cryptic FN-binding sites in matrix assembly, the conformational dynamics of III$_{1-2}$ must be characterized. One approach to this problem is to tag III$_{1-2}$ with fluorescent probes, which, in conjunction with fluorescent resonance energy transfer (FRET), create a molecular conformational sensor. FRET involves the radiationless transfer of energy from an excited donor fluorophore to an acceptor fluorophore, a process that is very sensitive to the distance between the two fluorophores (13–15). Two fluorescent protein variants, cyan fluorescent protein (CFP) and yellow fluorescent protein (YFP), are highly related to green fluorescent protein (GFP). Because the emission spectrum of CFP is well matched to the excitation spectrum of YFP, these two fluorophores have been widely used as a donor-acceptor pair in FRET studies (13–15).

In this study, we describe a FRET conformational sensor designed to test the idea that intramolecular interactions between III$_1$ and III$_2$ sequester key FN-binding and assembly sites. We show that III$_{1-2}$ with CFP and YFP fused to the N and C termini, respectively, displays a clear FRET signal, indicating that the attached fluorescent proteins and thus the ends of III$_{1-2}$ are in close proximity. FRET data from III$_{1-2}$ mutants support the presence of a stabilizing intermodule salt bridge that regulates FN-binding activity.

EXPERIMENTAL PROCEDURES

Production and Purification of CFP/YFP Fusion Proteins and SDS-PAGE—The enhanced CFP gene (pECFP, Clontech, Mountain View, CA) with a Gly-Ser-Gly-Ser-Gly coding sequence at the 3′-end and BamHI and BglII restriction sites at the 5′- and 3′-ends, respectively, was generated by PCR

and cloned into the pGEM vector (Promega, Madison, WI) to generate pGEM-CFP. The CFP BamHI-BglII fragment of pGEM-CFP was inserted into the BamHI site of pGEX-6P-2 (GE Healthcare) upstream of human III$_{1-2}$ to generate the donor-only construct CFP-III$_{1-2}$ in pGEX or CIII. The gene expressing III$_{1-2}$-YFP with BamHI and EcoRI restriction sites at the 5'- and 3'-ends, respectively, was created by overlap extension PCR. Overlap PCR consisted of a first PCR with primers flanking the termini of the FN III$_{1-2}$ domain in pGEX-6P-2 but excluding the stop codon at the 3'-end and primers flanking YFP in pEYFP (Clontech) including the YFP stop codon. The second PCR used the two PCR products from the first reaction and the aforementioned 5'-primer of the III$_{1-2}$ domain and the 3'-primer of pEYFP. The final PCR product was cloned into the pGEM vector to generate pGEM-YFP, which was subsequently cloned into the BamHI and EcoRI sites of pGEX-6P-2 to generate the acceptor-only gene, III$_{1-2}$-YFP or IIIY. The donor-acceptor construct, CFP-III$_{1-2}$-YFP or CIIIY, was created by ligating the BamHI-CFP-BglII fragment from pGEM-CFP to the BamHI site of the acceptor-only construct IIIY. All of the constructs were expressed as glutathione *S*-transferase (GST) fusion proteins in *Escherichia coli* DH12α. Mutants CIIIYK669A and CIIIYD767A, with alanine substitutions at FN residues Lys^{669} and Asp^{767}, were created in a similar manner using mutant III$_{1-2}$ constructs kindly provided by Dr. Iain Campbell (Oxford University). Mutant CIIIY in which both Lys^{669} and Asp^{767} were mutated to alanine (CIIIYK669A/D767A) was created by overlap extension using primers overlapping the single mutations in mutant III$_{1-2}$ domains. Mutant CIIIYK672A was created by PCR with primers overlapping the mutation site and incorporating the coding sequence for the mutated residue. To create CIIIYK672A/D767A, we ligated pGEX-6P-2-CIIIYK672A at the BamHI and StuI sites and inserted this mutant fragment into the pGEX-6P-2-CIIIYD767A fragment ligated at the BamHI and StuI sites. Overlap PCR with primers corresponding to the Lys^{669} and Lys^{672} genes and Asp^{767} were used to create the pGEX-6P-2-CIIIYK669A/K672A/D767A triple mutant. The proteins were then purified by affinity chromatography on glutathione-Sepharose 4 Fast Flow (GE Healthcare) following the manufacturer's specifications. High concentration fractions were dialyzed into 50 mM Tris-HCl (pH 7.5), 150 mM NaCl, 1 mM EDTA, and 1 mM dithiothreitol. Following dialysis, Precision protease (GE Healthcare) was used to cleave off GST, which was then separated from III$_{1-2}$-containing proteins by affinity chromatography. Proteins were dialyzed into 50 mM Tris-HCl (pH 8.0), 50 mM NaCl, and 2 mM EDTA; flash frozen; and stored at −80 °C. Prior to use, the fusion proteins were thawed at 4 °C and spun at 13,000 rpm for 5 min.

The GFP and FN epitopes were immunodetected using mouse monoclonal antibodies JL-8 (BD Biosciences) and 5E6, respectively. JL-8 recognizes GFP and its variants such as CFP and YFP. Monoclonal antibody 5E6 was raised against a GST-III$_{1-2}$ fusion protein and is specific for human III$_{1-2}$. Proteins were separated by SDS-PAGE on a 10% polyacrylamide gel, transferred to Hybond ECL nitrocellulose membrane (Amersham Biosciences), and incubated with primary and secondary antibodies. Hybridoma culture supernatant containing anti-

body 5E6 was used at 1:100 dilution. Antibody JL-8 was diluted 1:2000 according to the manufacturer's recommendation. Horseradish peroxidase-conjugated goat anti-mouse IgG (Pierce) was used at a dilution of 1:10,000. Antibodies were detected with SuperSignal West Pico chemiluminescent reagents (Pierce).

Circular Dichroism Studies—CD spectra in the far-UV region (between 200 and 260 nm) were obtained using a J720 spectropolarimeter (Jasco, Easton, MD) in a 0.1-cm path length and at a temperature of 20 °C. A bandwidth of 2 nm and a scan rate of 50 nm/min were used. The ellipticities of III$_{1-2}$ and CIIIY were measured at concentrations of 3.5–5.0 μM in phosphate-buffered saline and in the presence of 0.5 and 2 M guanidinium chloride (GdmCl) in phosphate-buffered saline. Absorption spectra were collected in the range of 200–260 nm and converted to molar ellipticity, [θ], which is expressed in degrees/cm^2/dmol. Three scans were averaged for each individual sample.

FRET Measurements—Prior to FRET analysis, CFP/YFP fusion proteins were diluted to 100 nM in 50 mM Tris-HCl (pH 8), 50 mM NaCl, and 2 mM EDTA. Protein concentrations were determined and matched using the BCA protein assay (Pierce), the Bradford assay (Bio-Rad), optical density readings at 280 nm, and comparison of band intensities by SDS-PAGE and Coomassie blue staining. *In vitro* FRET measurements were carried out in a PTI photon-counting spectrofluorometer (Photon Technology International, Birmingham, NJ) equipped with a temperature-jacketed cuvette holder at 25 °C. Prior to sample analysis, the proteins were thawed and kept at 4 °C. Sample analysis was done by placing the protein solutions in a cuvette with a 1-cm path length, placing the cuvette in the holder, and equilibrating the protein solution to ambient temperature. An excitation wavelength of 433 nm was used for the FRET studies, and the steady-state emission profiles between 460 and 540 nm were determined by collecting the raw emission in duplicate, obtaining an average, and subtracting buffer emission.

Fluorescence emission was monitored under a variety of conditions. Steady-state and time course emissions at 475 and 525 nm, the CFP and YFP peaks, were monitored with 433 nm excitation of the FRET probes in the absence and presence of 3.2 μg of α-chymotrypsin (Sigma). As controls, emissions at 475 and 525 nm for CIII and IIIY, respectively, were monitored after protease addition and excitation at 433 nm for CIII and at 433 or 513 nm for IIIY. To analyze protease products, fusion proteins were cleaved with α-chymotrypsin for 100 s using the same mass ratio of protease to protein. Proteolysis was stopped with 1 mM phenylmethanesulfonyl fluoride (Sigma). The products of proteolysis were separated on a polyacrylamide gel and analyzed via immunoblotting with anti-GFP antibodies as described above. Sizes of cleavage products were determined from a plot of log molecular mass *versus* distance migrated relative to molecular mass markers. Steady-state emission profiles of CIIIY and controls were obtained in the absence and presence of GdmCl at concentrations of 0.5 and 2 M. Emission of CIIIY and its mutants at 475 and 525 nm was monitored during excitation at 433 nm in the absence and presence of 1.7 μM N-terminal 70-kDa FN fragment using the following procedure. Emission spectra at 475 and 525 nm were collected at

intervals of 1 s. After 20 s, the 70-kDa fragment was added to the cuvette, and emissions were continually monitored for 30 min, sufficient time for binding and conformational changes. Time-averaged emission data for the 15 s before the addition of the 70-kDa fragment and for the 15 s at 30 min of incubation were used to calculate initial and final FRET efficiencies. FRET efficiencies were calculated from donor peak emissions in the presence and absence of the 70-kDa fragment.

FRET efficiencies were calculated from the donor-side emission of intact and proteolytically cleaved samples (16). The FRET efficiency (E) is given in Equation 1,

$$E = 1 - \frac{D}{D_A} \qquad \text{(Eq. 1)}$$

where D and D_A are the values of the CFP emission peak in the donor-acceptor protein before and after cleavage, respectively.

Modeling of III$_{1-2}$ Conformation—An existing model of III$_{1-2}$ deposited into the Protein Data Bank (code 2HA1) by Vakonakis *et al.* (17) was altered to accommodate the FRET data. The Protein Data Bank file was modified to position Lys^{672} and Asp^{767} near each other as would occur in a salt bridge. In an alternative model, III$_2$ was reoriented ~180° with respect to III$_1$ while maintaining the Lys^{672}-Asp^{767} interaction. Only the lysine, aspartic acid, and glutamic acid residues were moved as rotamers, and gross packing errors were avoided.

RESULTS

Design and Characterization of a FRET Conformational Sensor—Fibronectin in solution has a compact conformation (18) but is converted into an extended form that participates in FN-FN interactions during fibril formation. We propose that, in soluble FN, III$_1$ and III$_2$ interact to sequester FN-binding sites that become exposed during FN extension and fibril assembly. A simplified model of how the conformation of III$_{1-2}$ may influence access to FN-binding sites is shown in Fig. 1*B* and is based on the following properties of III$_{1-2}$. FN type III repeats are β-barrel structures with a long axis of 35–40 Å and a lateral width of ~20 Å (19, 20). The isoelectric points for III$_1$ and III$_2$ are 9.45 and 3.79, respectively, suggesting the possibility that these modules may associate through electrostatic interactions. There is a 17-amino acid linker between III$_1$ and III$_2$ with the sequence STSTPVTSNTVTGETTP; the abundance of serine and threonine residues is characteristic of a flexible polypeptide chain (21). The contour length of a linear form of the backbone carbon atoms of the linker is ~50 Å, which is long enough to allow the two modules to interact. As proposed by our model, intramolecular interactions give III$_{1-2}$ a compact conformation within which FN-binding sites are sequestered (Fig. 1*B, panel i*). Conformational changes, perhaps induced by cell-derived tension (12, 22), could open up the domain and expose the FN-binding sites (Fig. 1*B, panel ii*).

This model predicts that the N terminus of III$_1$ and the C terminus of III$_2$ are close together in solution. To investigate this possibility, we developed a FRET-based conformational sensor. CFP and YFP were conjugated at the N and C termini of III$_{1-2}$, respectively, to create CIIIY (Fig. 1*C*). We employed a -GSGSG- spacer between the FN modules and the fluorophores
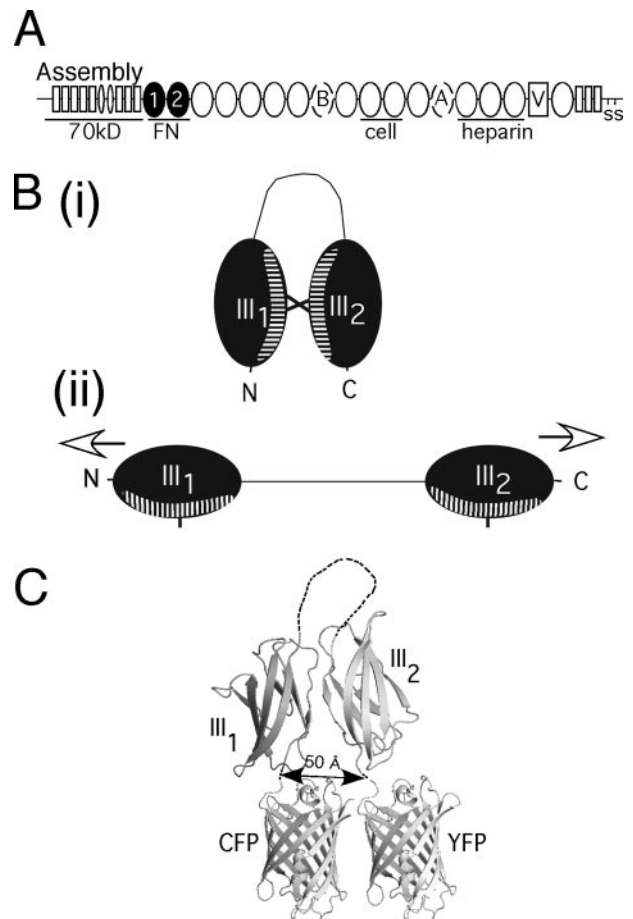

FIGURE 1. **The FN III$_{1-2}$ FRET conformational sensor.** *A*, representation of the domain structure of FN and major interaction sites. FN is composed of repeating modules that form binding domains for other FN molecules, cell receptors, and other extracellular matrix components as indicated. The first two type III modules III$_1$ and III$_2$ (*black*), have FN-binding sites and regulate FN matrix assembly. The N-terminal 70-kDa region contains a matrix assembly domain with FN-binding activity. The cell-binding domain (*cell*), the heparin-binding domain (*heparin*), the dimerization site (*SS*), and the alternatively spliced type IIIA (*A*), IIIB (*B*), and variable regions (*V*) are indicated. *70kD*, N-terminal 70-kDa FN fragment. *B*, schematic of proposed model of III$_{1-2}$ domain conformation. *Panel i*, in solution, the FN-binding sites in III$_1$ and III$_2$ (*hatched areas*) are sequestered through domain orientations that are facilitated by the linker between modules (*thin line*). *Panel ii*, binding sites are exposed through conformational changes resulting from cell-mediated extension of FN (*arrows*). The length of the linker and the height and width of the modules are drawn to scale for a linear peptide and published data on FN type III modules, respectively. *C*, ribbon diagram representation of CIIIY, a FRET sensor of the model in *B* (*panel i*), oriented with N and C termini 50 Å apart. CIIIY consists of the III$_{1-2}$ domain with CFP at the N terminus and YFP at the C terminus.

to provide a flexible connection between the fluorophores and the III$_{1-2}$ domain and to impart rotational mobility (23, 24). Considering the dimensions of type III modules, a distance estimate between N and C termini in this model is ~50 Å. The distance at which 50% of CFP energy is transferred to YFP, known as the Förster distance, is ~50 Å (25). The spectrofluorometer used in this study is capable of robustly measuring FRET efficiencies equal to or greater than 5%, which corresponds to a distance of 80 Å or less between the donor and acceptor fluorophores. Therefore, the distance between termini in our model is within the distance requirement for FRET to occur and be detected in CIIIY. In addition to the doubly labeled CIIIY protein, we also created a CIII donor-only variant
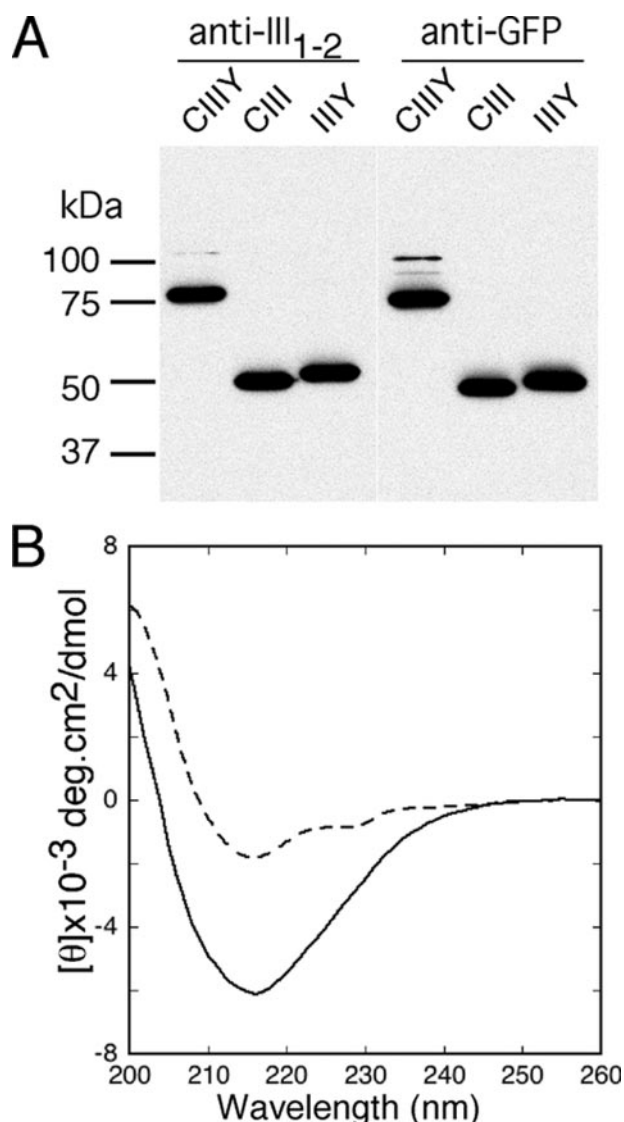
FIGURE 2. **Characterization of the CIIIY FRET probe.** *A*, purified CIIIY, CIII, and IIIY were separated on a SDS-10% polyacrylamide gel and probed with anti-III$_{1-2}$ (*left panel*) and anti-GFP (*right panel*) antibodies after GST tag removal. The molecular masses of CIIIY, CIII, and IIIY are 76.0, 49.5, and 49.7 kDa, respectively. The positions of the molecular mass markers are indicated on the left. The faint band at 100 kDa in the *CIIIY lanes* is uncleaved GST-CIIIY and represents <5% of the total protein in the preparation. *B*, CD spectra of CIIIY (——) and III$_{1-2}$ (– – –) are shown. *deg*, degrees.
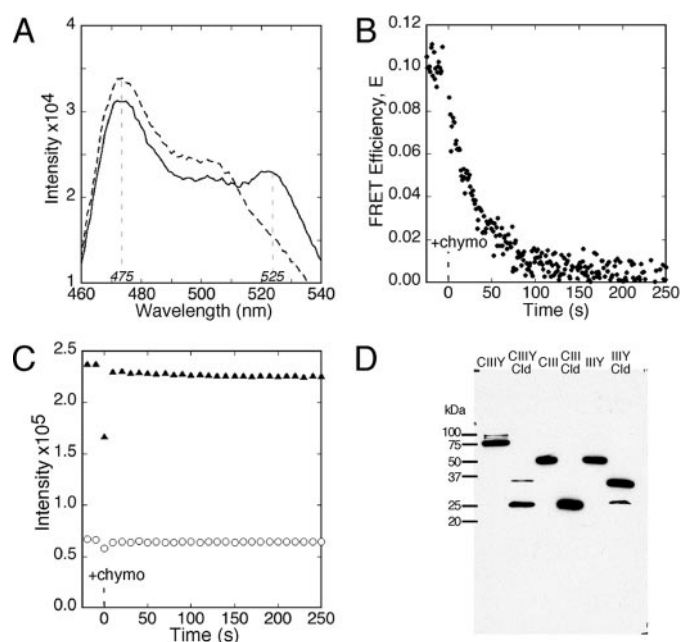

FIGURE 3. **Effects of proteolysis on FRET in CIIIY.** The fluorescence emission spectra of a 100 nM solution of proteins excited at 433 nm were collected between 460 and 540 nm in the absence and presence of 3.2 μg/ml of α-chymotrypsin. *A*, shown are the emission spectra of CIIIY (——) and cleaved CIIIY 15 min after α-chymotrypsin addition (– – –). The donor peak emission (475 nm) and acceptor peak emission (525 nm) are marked. *B*, shown is the time course of FRET efficiency of CIIIY following the addition of α-chymotrypsin at $t = 0$ (*+chymo*). *C*, shown are the time course CFP and YFP peak emission intensities for the controls CIII at 475 nm (▲) and IIIY at 525 nm (○) before and after protease addition (at $t = 0$; *+chymo*). Emission spectra of CIII and IIIY are plotted on the same graph but were collected separately after excitation at 433 nm. *D*, proteins were incubated with α-chymotrypsin for 100 s, separated on a SDS-15% polyacrylamide gel, and probed with anti-GFP antibodies. *CIIIY*, *CIII*, and *IIIY* indicate mock-treated proteins; *CIIIY Cld*, *CIII Cld*, and *IIIY Cld* indicate protease-treated proteins. Molecular mass standards are shown on the left.

with CFP conjugated to the N terminus of III$_{1-2}$ and a IIIY acceptor-only variant with YFP conjugated to the C terminus.

Purified fusion proteins were characterized by SDS-PAGE and immunoblotting with antibodies specific to either the III$_{1-2}$ or GFP moiety. FN and GFP epitopes were present in CIIIY, CIII, and IIIY, and all fusion proteins were of the expected sizes (Fig. 2*A*). Solid-phase binding assays showed that the N-terminal 70-kDa FN fragment bound similarly to immobilized CIIIY and III$_{1-2}$ (supplemental Fig. 1), indicating that FN binding was not perturbed by the addition of CFP and YFP.

The secondary structures of FN type III modules and of CFP and YFP are primarily β-sheet. In CD studies, CIIIY and III$_{1-2}$ were both characterized by a prominent negative peak at 215 nm, indicative of a β-sheet (Fig. 2*B*). The coincidence of the absorption peaks at 215 nm shows that CIIIY and III$_{1-2}$ have

similar secondary structures. However, CIIIY has a peak value of -6.12×10^3 degrees/cm^2/dmol, which is much larger than the III$_{1-2}$ peak at -1.80×10^3 degrees/cm^2/dmol (Fig. 2*B*). At 215 nm, the ellipticity of GFP, which has very similar secondary structure to CFP and YFP (26), is approximately -7.14×10^3 degrees/cm^2/dmol (27). A linear combination of the 215 nm absorption spectra of two GFP molecules and III$_{1-2}$ gives a molar ellipticity of -5.54×10^3 degrees/cm^2/dmol, which is comparable with our experimental value for CIIIY. Thus, the secondary structure of CIIIY does not vary significantly from its constituents CFP, YFP, and III$_{1-2}$. There is a secondary minimum at 230 nm in the trace for III$_{1-2}$, which does not correspond to known secondary structure profiles. This secondary minimum may be due to an unstructured domain such as the flexible linker that may be masked by the contributions from CFP and YFP in the CIIIY spectrum.

Intramolecular FRET in CIIIY—Fluorescence spectroscopy studies of CIIIY demonstrated a strong FRET signal between the CFP and YFP moieties. CFP excitation in CIIIY resulted in emission peaks at 475 and 525 nm (Fig. 3*A*), corresponding to CFP and YFP emission peaks, respectively. The detection of sensitized YFP emission upon excitation at 433 nm strongly suggests that the CFP and YFP probes in the CIIIY construct are sufficiently close together for FRET. To validate this finding, we

employed several strategies designed to disrupt the close proximity of the FRET probes.

Proteolytic sites for α-chymotrypsin exist in III$_{1-2}$ (11), whereas the CFP/YFP fluorophores are resistant to protease digestion (reviewed in Ref. 26). The addition of α-chymotrypsin to CIIIY resulted in a dramatic loss of sensitized YFP emission and a dequenching of the CFP emission indicated by increased peak height at 475 nm (Fig. 3*A*). These changes are highly consistent with efficient energy transfer in the intact CIIIY molecule. The transfer efficiency in intact CIIIY, calculated using Equation 1 (see "Experimental Procedures"), gives a FRET efficiency of 0.10 in CIIIY. A similar value of FRET efficiency was obtained using 10 and 50 nM solutions of CIIIY, indicating that FRET efficiency was independent of protein concentration (data not shown). Because GFP fluorescence is sensitive to changes in the environment (26), which may change with time during proteolysis, we examined how fluorescence emission in CIIIY and in the controls changed with time during proteolysis. Time course analysis of CIIIY proteolysis confirmed a decrease in FRET efficiency with increasing cleavage time in the presence of the protease (Fig. 3*B*). After protease addition to control proteins, the 475 nm emission peak intensity of the donor-only CIII and the 525 nm peak emission intensity of IIIY after 433 nm excitation did not change (Fig. 3*C*), confirming their resistance to cleavage. We also observed no difference in the acceptor peak intensity in IIIY when directly exciting YFP at 513 nm (data not shown). Proteolytic products were examined after 100 s, the time it took to eliminate FRET in Fig. 3*B*. Immunoblotting with anti-GFP antibodies identified proteolytic fragments with molecular masses of 37 and 27 kDa (Fig. 3*D*). CIIIY cleavage products correspond to fragments generated by cleavage of the donor-only (CIII) and acceptor-only (IIIY) proteins. No fragments smaller than 27 kDa were detected. The 27-kDa fragment is approximately the size of CFP or YFP, suggesting cleavage at the interface between III$_{1-2}$ and the fluorophore, whereas the 37-kDa fragment contains fluorophore and a portion of III$_{1-2}$. Therefore, the loss of FRET and the increased distance between the donor and acceptor fluorophores result from CIIIY proteolysis. These results demonstrate the presence of intramolecular FRET in intact CIIIY.

In a second strategy, we treated CIIIY with GdmCl because this denaturant has been shown to disrupt intramolecular interactions and gradually transform full-length FN from a compact to an extended conformation (28). In 2 M GdmCl, fluorescence emission and CD spectroscopy showed FN in an extended conformation, but the secondary structure within its modules remained intact (28). On the other hand, GFP fluorophores are stable and fluorescent at concentrations of GdmCl up to 6 M (29). We monitored the effect of 0.5 and 2 M GdmCl on FRET in CIIIY. The emission of CIIIY in 0.5 M GdmCl was characterized by a reduction of the YFP emission peak compared with its emission in a nondenaturing solution (Fig. 4*A*). Interestingly, the CD spectra of CIIIY and III$_{1-2}$ in 0.5 M GdmCl were comparable with those in a nondenaturing solution (Fig. 4, *B* and *C*), indicating that the secondary structure of III$_{1-2}$ was not perturbed by 0.5 M GdmCl. When the concentration of GdmCl was increased from 0.5 to 2 M, the YFP emission peak was eliminated from the emission spectra of CIIIY excited at
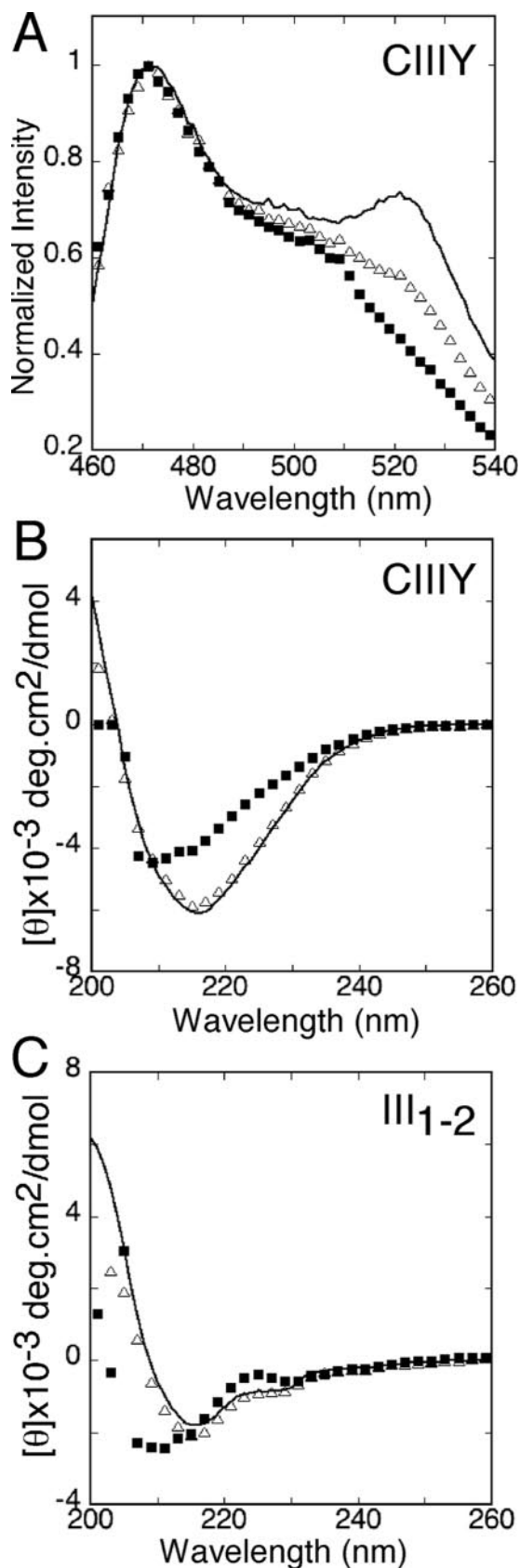

FIGURE 4. **Increasing denaturant concentration leads to loss of FRET in CIIIY.** *A*, normalized emission spectra relative to the peak of CFP emission at 475 nm of CIIIY in 0 (——), 0.5 (△), and 2 (■) M GdmCl during excitation at 433 nm. *B* and *C*, far-UV CD spectra of CIIIY and III$_{1-2}$, respectively, in 0 (——), 0.5 (△), and 2 (■) M GdmCl. *deg*, degrees.

433 nm (Fig. 4*A*). The CD spectra of CIIIY and III$_{1-2}$ in 2 M GdmCl were distinct from those in 0.5 M GdmCl (Fig. 4, *B* and *C*) and were marked by a shift in the minima to lower wavelengths, reflecting a loss of β-sheet structure. The maintenance of β-sheet structure with the loss of FRET in the 0.5 M GdmCl environment confirms the disruption of intramolecular interactions between the FN modules in III$_{1-2}$. These CD and FRET studies in the absence and presence of varying denaturant concentrations are indicative of III$_{1-2}$ structural transitions in the different environments: a compact III$_{1-2}$ domain in the absence of denaturant, a partially open III$_{1-2}$ domain with intact secondary structure in the FN modules in 0.5 M GdmCl, and a fully open III$_{1-2}$ domain with some loss of secondary structure in 2 M GdmCl.

Mutations in III$_{1-2}$ Influence FRET and FN Binding—The conformation of III$_{1-2}$ is proposed to be stabilized by a salt bridge between Lys[669] in III$_1$ and Asp[767] in III$_2$ (17). We used FRET to probe the conformation of CIIIY mutants with alanine residues in place of Lys[669] and Asp[767] (CIIIYK669A/D767A). FRET in CIIIYK669A/D767A was characterized by an increase in the acceptor peak of the donor normalized data or the I_A/I_D value (Fig. 5*A*), indicating that the N and C termini are closer together in the mutant. A time course analysis of changes in FRET efficiency in CIIIYK669A/D767A in the presence of α-chymotrypsin confirmed the presence of intramolecular FRET (Fig. 5*B*). Intact CIIIYK669A/D767A had a higher FRET efficiency than intact CIIIY (0.19 *versus* 0.10). Furthermore, the effect of α-chymotrypsin on CIIIYK669A/D767A was similar to its effect on CIIIY, causing a 50% reduction in FRET efficiency within 30 s of protease addition (see Fig. 3*B*). Thus, the rates of proteolysis in CIIIY and CIIIYK669A/D767A were comparable, suggesting that the mutations did not cause any major structural changes. However, the increase in FRET efficiency from 0.10 in CIIIY to 0.19 in CIIIYK669A/D767A strongly supports the conclusion that one or both of these mutations induce subtle conformational changes in III$_{1-2}$ that reduce the distance between the N and C termini.

Analysis of the single mutant CIIIYD767A showed acceptor emission similar to that of CIIIYK669A/D767A as represented by the acceptor peak enhancement of the donor normalized data I_A/I_D (Fig. 5*C*). In contrast, the emission profile of CIIIYK669A was comparable with that of wild-type CIIIY. Thus, mutation of Asp[767] impacted III$_{1-2}$ conformation, whereas the K669A mutation did not. Furthermore, the single mutant results show that the increased FRET efficiency of CIIIYK669A/D767A (Fig. 5, *A* and *B*) is due to D767A. Examination of III$_{1-2}$ sequence alignment from different species shows a highly conserved Lys[672] residue (17). A CIIIY FRET probe containing K672A had a significant increase in the I_A/I_D value, comparable with that observed in CIIIYD767A (Fig. 5*C*). The similarity in FRET changes with mutation of either Lys[672] or Asp[767] strongly suggests that these two residues are associated in CIIIY. This interpretation is further supported by the triple mutant CIIIYK669A/K672A/D767A, which also had increased FRET compared with CIIIY and CIIIYK669A.

The double mutant CIIIYK672A/D767A displayed a FRET efficiency that was similar to that of CIIIYD767A ($\sim$0.18) (Fig. 5*D*). However, its I_A/I_D value was comparable with that of CIIIY
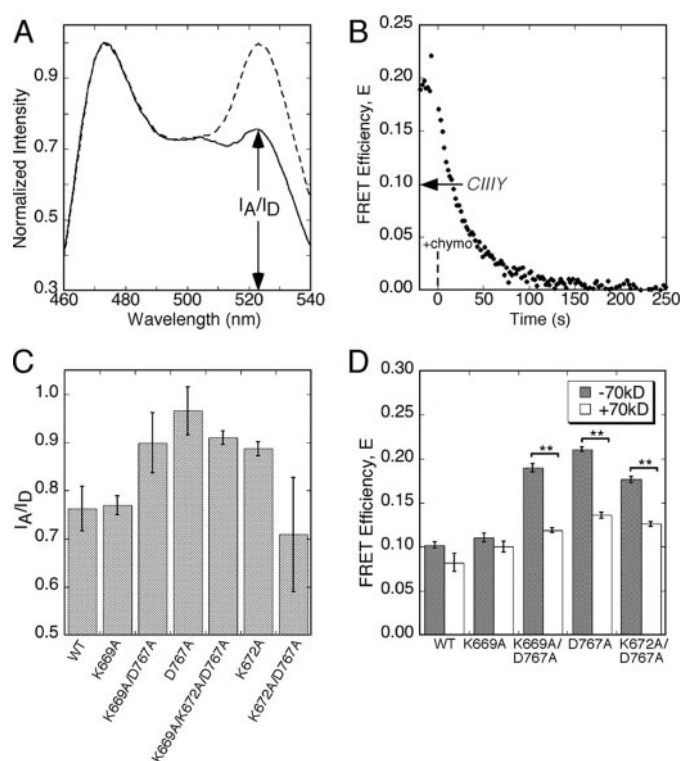

FIGURE 5. **Effects of mutations on FRET and on N-terminal 70-kDa FN fragment binding.** *A*, normalized emission spectra relative to the peak of CFP emission at 475 nm of CIIIY (——) and CIIIYK669A/D767A (– – –). The marked I_A/I_D value (the ratio of the acceptor to the donor peak) was used for comparing FRET efficiencies of CIIIY with those of its mutants in *C*. *B*, FRET efficiencies in CIIIYK669A/D767A as a function of time following the addition of 3.2 μg/ml α-chymotrypsin to a 100 nM solution. The efficiency of intact CIIIY and the time point for protease addition (+*chymo*) are indicated. *C*, I_A/I_D values calculated for CIIIY (wild-type (*WT*)) and its mutants as indicated. *Error bars* represent a 95% confidence interval of data from three repeats. *D*, FRET efficiencies in CIIIY (wild-type) and in mutants CIIIYK669A, CIIIYK669A/D767A, CIIIYD767A, and CIIIYK672A/D767A in the absence (*gray bars*) and presence (*white bars*) of the 70-kDa fragment (*70kD*). *E* was calculated from emission data collected before the addition of the 70-kDa fragment and at 30 min of incubation with the 70-kDa fragment. Measurements represent means $\pm$ S.E. of the mean of the time-averaged data. **, $p < 0.001$.

(Fig. 5*C*). FRET efficiencies are evaluated from the donor side, and the high efficiency in CIIIYK672A/D767A supports a conformational change similar to that of the single mutant. The low I_A/I_D value for the double mutant suggests that there may be an unidentified defect in the acceptor fluorophore. Nonetheless, the increased FRET efficiency in CIIIYK672A/D767A, as well as the increases in acceptor emission in either single mutant and in CIIIYK669A/K672A/D767A, supports an interaction between Lys[672] and Asp[767] in III$_{1-2}$.

To determine whether the conformational differences that increase the FRET signal affect the FN-binding activity of III$_{1-2}$, we examined the emissions of CIIIY and its mutants in the presence and absence of the N-terminal 70-kDa FN-binding fragment (see Fig. 1*A*). Mutation of Asp[767] alone or in combination with Lys[672] induced significant increases in FRET efficiencies similar to CIIIYK669A/D767A (Fig. 5*D*). The addition of the 70-kDa fragment led to a significant loss of FRET efficiency in CIIIYD767A, CIIIYK669A/D767A, and CIIIYK672A/D767A but had no significant effect on the FRET signal in CIIIY and CIIIYK669A (Fig. 5*D*). In the presence of the 70-kDa fragment, the FRET efficiencies of CIIIYD767A, CIIIYK669A/
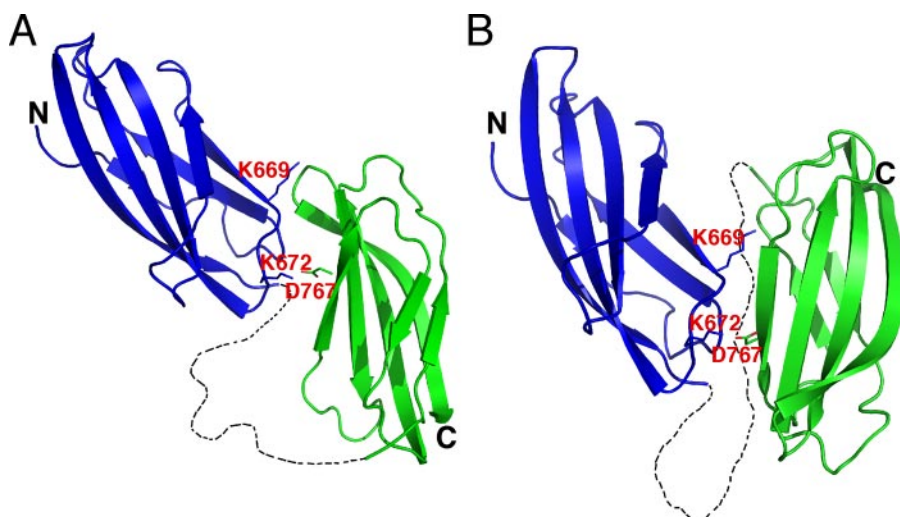
FIGURE 6. **Two possible FN module orientations in III$_{1-2}$.** *A*, the orientation of FN modules is similar to that of Vakonakis *et al.* (17) but with a Lys^{672}-Asp^{767} interaction instead of a Lys^{669}-Asp^{767} interaction. *B*, the orientation of III$_2$ is rotated ~180° relative to *A* while maintaining the Lys^{672}-Asp^{767} salt bridge.

FRET efficiency of 0.10 in CIIIY corresponds to a distance between CFP and YFP that is 70 Å or less. A model of III$_{1-2}$ based on NMR solution structures of the individual modules, III$_1$ (19, 32) and III$_2$ (17), predicts a distance of 60 Å between the N and C termini (17), comparable with the estimate from our FRET analyses. Thus, these two independent approaches are in agreement with regard to a compact conformation of III$_{1-2}$.

A salt bridge between Lys^{669} in III$_1$ and Asp^{767} in III$_2$ has been proposed by Vakonakis *et al.* (17). However, the interaction between III$_1$ and III$_2$ was not disrupted in their K669A mutant compared with the native protein. On the other hand, a D767A mutation perturbed interactions between III$_1$ and III$_2$ (17). We have also found, using FRET analyses, that replacement of Asp^{767} with alanine had a significant effect on III$_{1-2}$ conformation and on binding to the 70-kDa FN fragment. In contrast, K669A had no effect on either conformation or 70-kDa fragment binding. With D767A, we detected a 10-Å decrease in the distance between N and C termini. Interestingly, similar changes in the distance between the domain ends and in 70-kDa fragment binding were obtained with the K672A mutation. The effects on III$_{1-2}$ conformation and FN binding of K672A and D767A, but not K669A, indicate that Lys^{672} and Asp^{767} play similar roles in positioning N and C termini relative to each other and suggest that these two residues form a salt bridge.

These FRET data provide independent measures of the distance between the ends of III$_{1-2}$ and the residues that are significant in module interactions. This information can be combined with existing structural models to provide insights into III$_{1-2}$ conformation. Working with a published model (17), we propose two possible III$_{1-2}$ conformations. In both models, a Lys^{672}-Asp^{767} salt bridge has a pivotal role, and a compact III$_{1-2}$ conformation is maintained. The major difference is in the orientations of III$_2$ relative to III$_1$. The first model shown in Fig. 6*A* is similar to that of Vakonakis *et al.* (17), with N and C termini extended in opposite directions but with III$_2$ shifted somewhat to facilitate a Lys^{672}-Asp^{767} interaction. In the second model, the orientation of the modules has been changed. III$_2$ was rotated 180° relative to its position in Fig. 6*A* using Lys^{672}-Asp^{767} as a pivot; N and C termini point in approximately the same direction in this model (Fig. 6*B*). The positions of the flexible linker region are quite different between the two models. However, there is overlap in the residues that constitute the III$_1$-III$_2$ intermodule interface, and Lys^{669} is in the vicinity of acidic residues in III$_2$ in both orientations. These models provide a framework for further structural and mutational analyses to determine the exact interactions between these modules.

D767A, and CIIIYK672A/D767A decreased by ~55, 60, and 40%, respectively. Increases in FRET efficiency with mutation of Lys^{672}, Asp^{767}, or both support the conclusion that these two residues interact via a salt bridge in CIIIY and that disruption of this salt bridge induces conformational changes in III$_{1-2}$. The changes in FRET induced by the 70-kDa fragment suggest that the mutations expose a FN-binding site in III$_{1-2}$ and that binding to this site induces further conformational changes. No changes were observed with CIIIYK669A, further indicating that this residue is not directly involved in these intermodule interactions.

DISCUSSION

The III$_{1-2}$ domain of FN, containing two FN-binding sites, plays a regulatory role in matrix assembly. Using a FRET-based sensor of structural dynamics, we have shown here that opposite ends of III$_{1-2}$ are in close proximity rather than extended in opposite directions, as are other type III module pairs (30). The compact conformation of III$_{1-2}$ was disrupted by mild denaturation that separated N and C termini but did not perturb the β-barrel secondary structures of the individual modules. The conformation of CIIIY was also altered by mutation of Lys^{672} in III$_1$ or Asp^{767} in III$_2$. Binding of the 70-kDa FN matrix assembly fragment to mutant CIIIY caused a dramatic reduction in FRET, demonstrating that FN-FN interactions affect the conformation of the III$_{1-2}$ domain. These results provide new insights into the distance between the ends of III$_{1-2}$ and the nature of intramolecular interactions in this domain that keep it in a compact state.

We have used GFP-based FRET spectroscopy to assign a distance limit between the two fluorophores and to get an estimate of the distance between the N and C termini of III$_{1-2}$. FRET efficiency depends on the orientation of the CFP and YFP fluorophores with respect to each other. Although the precise orientation of the two fluorophores is unknown, it is possible to obtain an upper limit of the distance between them from the Förster distance of the FRET pair (31). A

FRET Study of Fibronectin III$_{1-2}$ Conformation

The interaction of the 70-kDa fragment with the D767A single and double mutants leads to an increase in the distance between the N and C termini of III$_{1-2}$. This finding confirms an interaction between the matrix assembly domain of FN and III$_{1-2}$. As III$_{1-2}$ has both native and cryptic FN-binding sites, this change in conformation may result in exposure of another binding site for FN or for other extracellular matrix components in III$_{1-2}$. The III$_{1-2}$ domain has been implicated in formation of stable detergent-insoluble FN fibrils. The regulated exposure of binding sites through 70-kDa fragment binding may be critical for development of stable matrix. Moreover, the potential to bind to more than one FN molecule raises the possibility that III$_{1-2}$ may act as a branching point for new FN fibrils.

REFERENCES

1. Mao, Y., and Schwarzbauer, J. E. (2005) *Matrix Biol.* **24,** 389–399
2. Ghosh, K., Ren, X. D., Shu, X. Z., Prestwich, G. D., and Clark, R. A. (2006) *Tissue Eng.* **12,** 601–613
3. Honest, H., Bachmann, L. M., Gupta, J. K., Kleijnen, J., and Khan, K. S. (2002) *Br. Med. J.* **325,** 301
4. Santimaria, M., Moscatelli, G., Viale, G. L., Giovannoni, L., Neri, G., Viti, F., Leprini, A., Borsi, L., Castellani, P., Zardi, L., Neri, D., and Riva, P. (2003) *Clin. Cancer Res.* **9,** 571–579
5. Aguirre, K. M., McCormick, R. J., and Schwarzbauer, J. E. (1994) *J. Biol. Chem.* **269,** 27863–27868
6. Hocking, D. C., Sottile, J., and McKeown-Longo, P. J. (1994) *J. Biol. Chem.* **269,** 19183–19187
7. Ingham, K. C., Brew, S. A., Huff, S., and Litvinovich, S. V. (1997) *J. Biol. Chem.* **272,** 1718–1724
8. Sechler, J. L., Rao, H., Cumiskey, A. M., Vega-Colon, I., Smith, M. S., Murata, T., and Schwarzbauer, J. E. (2001) *J. Cell Biol.* **154,** 1081–1088
9. Chernousov, M. A., Faerman, A. I., Frid, M. G., Printseva, O. Y., and Koteliansky, V. E. (1987) *FEBS Lett.* **217,** 124–128
10. Chernousov, M. A., Fogerty, F. J., Koteliansky, V. E., and Mosher, D. F. (1991) *J. Biol. Chem.* **266,** 10851–10858
11. Morla, A., and Ruoslahti, E. (1992) *J. Cell Biol.* **118,** 421–429
12. Zhong, C., Chrzanowska-Wodnicka, M., Brown, J., Shaub, A., Belkin, A. M., and Burridge, K. (1998) *J. Cell Biol.* **141,** 539–551
13. Miyawaki, A. (2003) *Dev. Cell* **4,** 295–305
14. Miyawaki, A., Sawano, A., and Kogure, T. (2003) *Nat. Cell Biol.* **5,** S1–S7
15. Tsien, R. Y. (1998) *Annu. Rev. Biochem.* **67,** 509–544
16. Epe, B., Steinhauser, K. G., and Woolley, P. (1983) *Proc. Natl. Acad. Sci. U. S. A.* **80,** 2579–2583
17. Vakonakis, I., Staunton, D., Rooney, L. M., and Campbell, I. D. (2007) *EMBO J.* **26,** 2575–2583
18. Johnson, K. J., Sage, H., Briscoe, G., and Erickson, H. P. (1999) *J. Biol. Chem.* **274,** 15473–15479
19. Briknarova, K., Akerman, M. E., Hoyt, D. W., Ruoslahti, E., and Ely, K. R. (2003) *J. Mol. Biol.* **332,** 205–215
20. Leahy, D. J., Aukhil, I., and Erickson, H. P. (1996) *Cell* **84,** 155–164
21. Argos, P. (1990) *J. Mol. Biol.* **211,** 943–958
22. Ohashi, T., Kiehart, D. P., and Erickson, H. P. (1999) *Proc. Natl. Acad. Sci. U. S. A.* **96,** 2153–2158
23. Prescott, M., Nowakowski, S., Nagley, P., and Devenish, R. J. (1999) *Anal. Biochem.* **273,** 305–307
24. Zhang, B. (2004) *Biochem. Biophys. Res. Commun.* **323,** 674–678
25. Patterson, G. H., Piston, D. W., and Barisas, B. G. (2000) *Anal. Biochem.* **284,** 438–440
26. Zimmer, M. (2002) *Chem. Rev.* **102,** 759–781
27. Visser, N. V., Hink, M. A., Borst, J. W., van der Krogt, G. N., and Visser, A. J. (2002) *FEBS Lett.* **521,** 31–35
28. Khan, M. Y., Medow, M. S., and Newman, S. A. (1990) *Biochem. J.* **270,** 33–38
29. Tsumoto, K., Umetsu, M., Kumagai, I., Ejima, D., and Arakawa, T. (2003) *Biochem. Biophys. Res. Commun.* **312,** 1383–1386
30. Campbell, I. D., and Spitzfaden, C. (1994) *Structure* **2,** 333–337
31. Lakowicz, J. (2006) *Principles of Fluorescence Spectroscopy*, Springer-Verlag New York Inc., New York
32. Gao, M., Craig, D., Lequin, O., Campbell, I. D., Vogel, V., and Schulten, K. (2003) *Proc. Natl. Acad. Sci. U. S. A.* **100,** 14784–14789

Probing the Conformation of the Fibronectin III$_{1-2}$ Domain by Fluorescence Resonance Energy Transfer

Nancy W. Karuri, Zong Lin, Hays S. Rye and Jean E. Schwarzbauer

Access the most updated version of this article at doi: 10.1074/jbc.M805025200

Alerts:
- When this article is cited
- When a correction for this article is posted

Click here to choose from all of JBC's e-mail alerts

Supplemental material:
http://www.jbc.org/content/suppl/2008/12/09/M805025200.DC1

This article cites 31 references, 14 of which can be accessed free at
http://www.jbc.org/content/284/6/3445.full.html#ref-list-1